

## SYNTHESIS AND EVALUATION OF QUINOLINE AND PIPERIDINE DERIVATIVES AS EHMT2 INHIBITORS: PROSPECTS FOR ANTIMALARIAL DRUG DEVELOPMENT

Moussa Toure<sup>1</sup>, Oumar Sambou<sup>1</sup>, Abdoulaye Gassama<sup>1,2\*</sup>, Christian Cave<sup>2</sup> and Sandrine Cojean<sup>2,3</sup>

<sup>1</sup>Laboratory of Chemistry and Physics of Materials (LCPM), Assane SECK University Ziguinchor, BP 523, Ziguinchor, Senegal.

<sup>2</sup>Antiparasitic Chemotherapy, UMR 8076 CNRS BioCIS, Paris-Sud University, Paris-Saclay University, 17 rue avenue des sciences, 91400 Orsay, France.

<sup>3</sup>National Malaria Reference Center, Hôpital Bichat-Claude Bernard, APHP, 75018 Paris, France.

\*Corresponding Author: Pr. Abdoulaye Gassama

Laboratory of Chemistry and Physics of Materials (LCPM), Assane SECK University Ziguinchor, BP 523, Ziguinchor, Senegal.

Article Received on 25/08/2023

Article Revised on 15/09/2023

Article Accepted on 05/10/2023

### ABSTRACT

In this study, we report the synthesis of a set of quinoline and piperidine derivatives and the *in vitro* evaluation of their antimalarial activity against chloroquine-sensitive (Pf3D7) and chloroquine-resistant (PfW2) *P. falciparum* strains. The *in vitro* cytotoxicity of these compounds was assessed to determine their impact on human cells. Preliminary *in vitro* results showed that these compounds displayed selective cytotoxicity and potent activity against both strains. In particular, compound **8** showed promising activity, with  $CI_{50}$  values of 1.36  $\mu$ M for strain 3D7 and 6.57  $\mu$ M for strain W2. An *in silico* approach was used in parallel, such as molecular docking and pharmacological and pharmacokinetic properties prediction (ADME) to study the ability of these compounds to bind to the target of interest and to predict their efficacy and safety in the context of oral administration.

**KEYWORDS:** antimalarial, *Plasmodium falciparum*, *in vitro*, *in silico*, quinoline, piperidine.

### INTRODUCTION

Malaria is a potentially fatal parasitic disease affecting millions of people worldwide.<sup>[1]</sup> It is mainly caused by parasites of the genus *Plasmodium*, transmitted to humans by the bites of infected female Anopheles mosquitoes.<sup>[2]</sup> The emergence and spread of resistance to artemisinin and its related drugs<sup>[3,4]</sup> - the most widely used combination of antimalarial drugs<sup>[5]</sup> - threaten to wipe out gains and could have devastating consequences worldwide. This calls for the urgent development of new therapeutic agents with distinct modes of action to overcome resistance and control multi-resistant *Plasmodium* parasites.<sup>[6]</sup>

Quinolines are heterocycles that have emerged as a promising class of compounds with significant antimalarial activity.<sup>[7,8]</sup> Aminoquinoline derivatives with amide function play a key role in interaction with target receptors or enzymes,<sup>[9]</sup> which may influence their pharmacological activity.<sup>[10]</sup> A number of organic and natural products containing peptide bonds possess interesting biological activities.<sup>[9]</sup> For this reason, the development of new peptide bonds containing the quinoline ring using simple reactions has become a fascinating area of research.

As part of our research into antimalarial quinoline derivatives, the present study focuses on the synthesis of *N*-benzyl-*N*-(8-quinolyl)-2-phenoxyacetamide analogues, containing an amide linkage (-CONR-), using an approach based on alkylation and acylation reactions starting from aminoquinoline and acyl chloride. We carried out an *in vitro* biological evaluation of the antimalarial activity of these compounds. In addition, cell viability tests were carried out to determine the effect of the compounds on cell survival (HUVEC).

An *in silico* study was also carried out on the ADME (Absorption Distribution Metabolism and Elimination) properties of the synthesized compounds, enabling us to estimate the ADME properties of the compounds, such as their intestinal absorption, solubility, metabolic stability and bioavailability.

Molecular docking appears to be an important and necessary step in understanding the process of biological reactions and in drug design. We performed molecular docking with proteins of interest involved in malaria, in order to predict the binding affinity of compounds and understand their potential mechanism of action. The Molecular Operating Environment (MOE), an open

access software package, was used to dock our compounds.<sup>[11]</sup>

## MATERIALS AND METHODES

### General

NMR spectra <sup>1</sup>H and <sup>13</sup>C were recorded at room temperature on a BRUKER UltraShield 300 spectrometer and tetramethylsilane (TMS) was used as internal reference. Analyses <sup>1</sup>H were obtained at 300 MHz and analyses <sup>13</sup>C were obtained at 75 MHz. Chemical shifts  $\delta$  are expressed in parts per million relatives to TMS ( $\delta = 0.00$ ). Different deuterated solvents were used depending on the solubility of the products. For <sup>1</sup>H spectra, the abbreviations s, d, t, q, dd and m refer to signals in singlet, doublet, triplet, quadruplet, split doublet and multiplet form. Coupling constants J are expressed in Hertz (Hz). Mass spectroscopy analyses were carried out on a Waters Micromass Quattro quadrupole/Q-TOF time-of-flight instrument equipped with ESI electrospray ionization or APCI atmospheric pressure chemical ionization. Reactions were monitored by Macherey-Nagel Polygram Sil G/UV<sub>254</sub> silica gel thin-layer chromatography (TLC) and products were detected under ultraviolet illumination at 254 nm. Product purification by column chromatography was carried out on silica gel (Merck Kieselgel 60).

### General procedure for the synthesis of 3a-c

A mixture of 8-aminoquinoline **1** (500 mg, 3.47 mmol) and 10.40 mmol triethylamine (Et<sub>3</sub>N) in 20 mL THF was stirred for 30 min at room temperature. The corresponding acetyl chloride (1.5 equiv) was added dropwise to the reaction mixture at 0°C. The mixture was stirred for 3 h at room temperature. 20 mL of an aqueous solution of NaOH (10%) was added to the mixture. The aqueous phase was extracted with ethyl acetate (3x10 mL). The organic phases were washed with NaCl salt solution (20 mL), dried over Na<sub>2</sub>SO<sub>4</sub> and then concentrated, under reduced pressure. The residue obtained required further purification on column chromatography with the eluent cyclohexane/AcOEt ratio 7:3. The product was obtained as a white solid.

### General procedure synthesis for 5(a-d)

A mixture of *phenoxy-N*-(quinolin-8-yl)acetamide **2** (100 mg, 0.37 mmol) and 3 equivalents of *i*Pr<sub>2</sub>NEt is dissolved in 20 mL THF. After addition of 2 equivalents of the corresponding substituted benzyl bromide (0.9 mmol), the reaction mixture is kept under stirring at room temperature for 24 to 48 hrs. The solvent was removed and the residue soaked in 20 mL of an aqueous solution of NaHCO<sub>3</sub>. The aqueous phase was extracted with CH<sub>2</sub>Cl<sub>2</sub> (3 x 10 mL). The organic phases were dried over anhydrous Na<sub>2</sub>SO<sub>4</sub> and concentrated under reduced pressure. The residue obtained was purified by silica gel column chromatography with the eluent cyclohexane/ethyl acetate (6/4) to give compounds **5(a-d)** as a yellowish powder.

### Synthesis of N-[(3-bromobenzyl)quinolin-8-amine (6)

A mixture of 8-aminoquinoline **1** (3.5 mmol) and 3-bromobenzyl bromide **4** (5.25 mmol) was dissolved in acetonitrile (20 mL). Potassium carbonate (14 mmol) was added in excess and the mixture was stirred for 5 hours. The liquid was removed and the residue cooled in a basic solution of sodium bicarbonate. The aqueous phase was extracted three times with ethyl acetate. The organic phases are dried over Na<sub>2</sub>SO<sub>4</sub>. The solvents are evaporated under reduced pressure. The residue obtained is purified on a silica chromatography column using a mixture of ethyl acetate and petroleum ether (1/9) as eluent to give the product as a white solid.

### Synthesis of N-(3-bromobenzyl)-2-chloro-N-(8-quinolyl) benzamide (8)

In a round-bottomed flask, 100mg (0.32mmol) of N-[(3-bromobenzyl) quinolin-8-amine **6** and 100 $\mu$ L of DIPEA in 10ml THF were stirred for ½ hour. 81 $\mu$ L (0.64mmol) of 3-bromobenzyl bromide **2c** was added dropwise to the solution containing **6**. After stirring at room temperature for 24 hours, the reaction was concentrated and then quenched with saturated NaHCO<sub>3</sub>. The aqueous phase was extracted three times with ethyl acetate. The organic phase was dried over MgSO<sub>4</sub> and then concentrated in vacuo. The residue obtained was purified on a silica gel chromatography column with the eluent cyclohexane/ethyl acetate in the ratio 6:4 to give pure compound **8** as a brown solid.

### Synthesis of 1-Boc-4-(3,4-dichloroanilino) piperidine (11)

In a nitrogen fed reaction vessel 4-oxo-piperidine-1-carboxylic acid tert-butyl ester **9** (0.3g, 1.5 mmol) and 3,4-dichloro-phenylalanine **10** (0.20 g, 1.23 mmol) were dissolved in dichloroethane (15 ml) and acetic acid (1.2 eq). Sodium triacetoxyborohydride (1.4 eq) was added at room temperature. The reaction was stirred overnight and then poured into a sodium hydroxyd solution (10%). The water phase was shaken three times with ethyl acetate (EtOAc). The combined organic phase was dried over sodium sulfate, evaporated and purified by flash chromatography (DCM 100% and DCM/MeOH 9,8/0,2) giving pure compound.

### Synthesis of t-butyl 4-(3,4-dichloro-N-[(E)-3-phenylprop-2-enoyl]anilino)piperidine-1-carboxylate (12)

A mixture of **11** (50mg; 0.15 mmol) and diisopropylethylamine (0.3 mmol) is dissolved in dichloromethane (10 mL). Cinnamoyl chloride **2** (0.22 mmol) is added in excess and the mixture is stirred for 48 hours at room temperature. The reaction is concentrated and cooled in sodium bicarbonate solution. The aqueous phase is then extracted three times with ethyl acetate. The organic phase is washed with an aqueous solution saturated with NaCl (40 mL) and dried over MgSO<sub>4</sub>. The solvents are evaporated under reduced pressure. The residue obtained is purified on a silica chromatography

column using ethyl acetate/cyclohexane (3/7) as eluent to give the product as a white solid.

#### General procedure for the synthesis of 14a-c

A mixture of piperidine (3.25 mmol) and excess potassium carbonate (8 mmol) is dissolved in dichloromethane (10 mL). After 40 minutes stirring, corresponding acyl chloride (6.5 mmol) is added dropwise at 0°C. The mixture is stirred for 24 to 48 hours in the presence of 100 µL triethylamine at room temperature. The liquid is removed and the residue cooled with sodium bicarbonate solution. The aqueous phase is then extracted three times with ethyl acetate. The organic phase is washed with an aqueous solution saturated with NaCl (40 mL) and dried over Na<sub>2</sub>SO<sub>4</sub>. The solvents are evaporated under reduced pressure. The residue obtained is purified on a silica chromatography column using ethyl acetate/cyclohexane (3/7) as eluent to give the product as a white powder.

#### General procedure for the synthesis of 16a-b

A mixture of t-butyl 4-(aminomethyl)piperidine-1-carboxylate **15** (2.33 mmol) and excess triethylamine (5 mmol) is dissolved in THF (15 mL). After 30 minutes stirring, corresponding cinnamoyl chloride **2** (3.5 mmol) is added dropwise at 0°C. The mixture is stirred for 3 h at room temperature. The solvent is removed and the residue cooled with sodium bicarbonate solution. The aqueous phase is then extracted three times with dichloromethane. The organic phase is washed with an aqueous solution saturated with NaCl (30 mL) and dried over Na<sub>2</sub>SO<sub>4</sub>. Solvents are evaporated under reduced pressure. The residue obtained is purified on a silica chromatography column using ethyl acetate/cyclohexane (3/7) as eluent to give the product as a light yellow powder.

### BIOLOGICAL PROCEDURE

In vitro test for growth and proliferation of *P. falciparum*. The compounds were tested against parasites of the susceptible *P. falciparum* strain 3D7 and the resistant *P. falciparum* strain W2, using the two-day fluorescence-based SYBR Green I approach.<sup>[12]</sup> Parasites were grown under standard conditions with minor modifications at 2.5% hematocrit in RPMI 1640 medium with an initial parasitemia of 1%. Compounds and negative control were prepared by double dilution, in the range 0.098-100 µg/mL, in a 96-well flat-bottom plate to give a final volume in each well of.<sup>[13]</sup> After 48 h incubation, the plates were subjected to 3 freeze-thaw cycles to achieve complete hemolysis. The parasite lysis suspension was diluted 1:5 in SYBR Green I lysis buffer. Plates were then incubated for a further hour at room temperature in the dark and examined for relative fluorescence units per well using epRealplex Master.<sup>[14]</sup> IC<sub>50</sub> values of active compounds were calculated by non-linear regression using ICEstimator Server version 1.2.<sup>[15]</sup>

#### In vitro cytotoxicity test

HUVEC cells were cultured in RPMI 1640 medium supplemented with 10% fetal bovine serum and 1 mM L-glutamine and incubated in 5% CO<sub>2</sub> at 37°C. Host cell cytotoxicity was assessed using the SYBR Green I assay as previously described. HUVEC cells were seeded in a 96-well plate at 100,000 cells/well and incubated for 24 h to adhere. After discarding the old medium, cells were incubated in medium containing eight concentrations (0.78-100 µg/mL) of each extract in duplicate. After 48 h incubation, cells were visualized using an inverted microscope to check morphology or cell viability. The medium was then removed and replaced with SYBR Green I-free lysis buffer, and the plates subjected to 3 freeze-thaw cycles. The cell lysis suspension was diluted 1:2 in SYBR Green I lysis buffer. Incorporation of SYBR Green I into cellular DNA and IC<sub>50</sub> analysis were obtained as before.

#### IN SILICO STUDY

In silico drug similarity and ADME analysis

The SwissADME online server was used to predict drug similarity and ADME parameters.<sup>[16]</sup>

#### Molecular docking

The crystal structure of the human malaria drug target co-crystallized with SAH (PDB ID: 2O8J)<sup>[17]</sup> was extracted from the Protein Data Bank ([www.rcsb.org/pdb](http://www.rcsb.org/pdb)). The protein was prepared using Molecular Operating Environment (MOE) version 2015.10 software, eliminating all water molecules. All compounds were drawn and optimized by the MOE software, and the resulting molecules were saved in mdb (molecule data base) format. The protein was considered to be rigid, but the flexibility of the molecules was taken into account, so that all possible poses could be exploited.

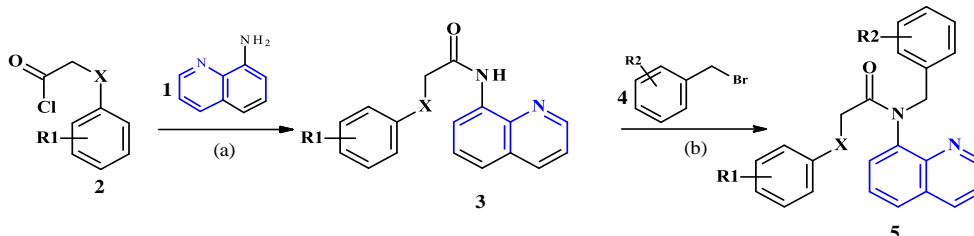
In MOE, receptor-ligand binding affinities with all possible binding geometries are prioritized on the basis of a numerical value called the S-score. Inhibitor interactions with receptor proteins are predicted on the basis of the S-score.<sup>[18]</sup> Docking results were manipulated using the GBVI/WSA dG scoring function with the generalized Born solvation model (GBVI). GBVI/WSA dG is a force-field-based scoring function that estimates the ligand's binding free energy from a given orientation.<sup>[19]</sup> The binding energy is directly associated with the conformation adopted by the ligand within the protein's active site. MOE's "Site Finder" module detects enzymatic cavities and the most favorable site in the protein.

The intermolecular interactions between the compounds and the G9a target (ID:2O8J) were visualized using Discovery Studio Visualizer software, providing insight into the molecular mechanisms underlying the compounds' activity.

## RESULTS AND DISCUSSION

## Chemistry

Quinoline-based amide analogues were synthesized by a simple two-step process according to **Scheme 1**. The method involves the reaction of activated carboxylic acid derivatives, such as chlorides, with amines.<sup>[20]</sup> Condensation of 8-aminoquinoline **1** with cinnamoyl chloride or phenoxyacetyl chloride led to precursors **3a-c**



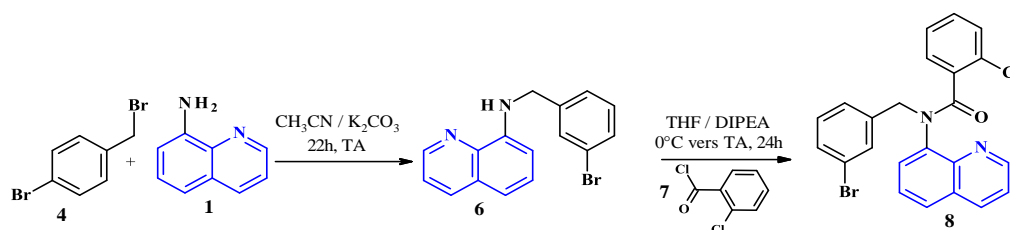
**Scheme 1.** Synthesis of quinoline analogues with a peptide bond. Conditions: (a) THF,  $\text{NET}_3$ , rt, 3h; (b)  $\text{CH}_3\text{CN}$ ,  $i\text{-Pr}_2\text{NEt}$ ,  $90^\circ$ , 24-48h

**Table 1:** Synthesized products derived from quinoline with the studied amide linkage.

Compound ID	R1	X	R2	Time (h)	Yield (%)
3a	H	O	/	3	99
3b	4-Br	O	/	3	90
3c	H	C=	/	3	88
5a	H	O	2-Br	4	69
5b	H	O	3-Br	4	60
5c	H	O	4-Br	4	70
5d	H	C=	4-F	48	75

Another quinoline analogue was synthesized in two steps, N-(3-bromobenzyl)-2-chloro-N-(8-quinoly)benzamide (**8**), in moderate yield. Thus, the amine of 8-aminoquinoline **1** was first alkylated by

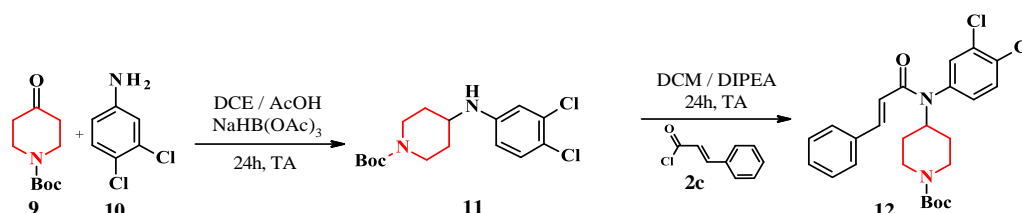
substituted benzyl bromide **4** to give the precursor **6** (monoalkylated). Acylation of **6** with 2-chlorobenzoyl chloride **7** in THF in the presence of DIPEA gave the desired compound **8** in 72% yield (**Scheme 2**).



**Scheme 2:** Synthesis of *N*-[3-bromobenzyl]-2-chloro-*N*-(8-quinoly)benzamide **8**.

For the synthesis of piperidine analogues, we modified a methodology adopted from the literature.<sup>21,22</sup> Accordingly, the key precursor **11** (rdt = 68%), was synthesized by reductive amination of condensing Boc-piperidone **9** with 3,4-dichloroaniline **10** in acid medium

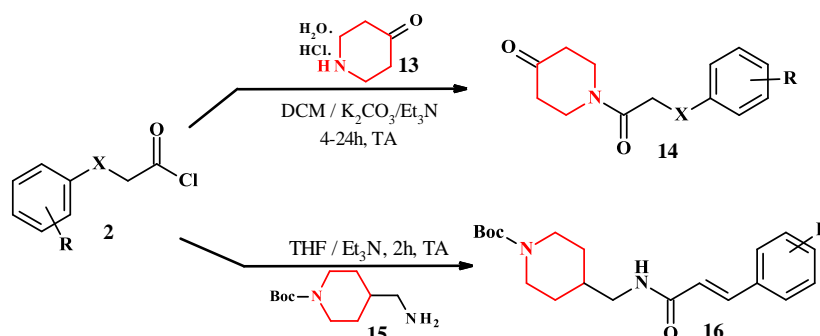
in the presence of sodium triacetoxyborohydride in dichloroethane. Compound **11** was then treated with cinnamoyl chloride **2c** to give the desired compound **12** in 28% yield (**Scheme 3**). It is therefore possible to screen other bases and solvents to optimize yield.



**Scheme 3:** Synthesis of *N*-(1-boc-piperidin-4-yl)-*N*-(3,4-dichloro-phenyl)-cinnamamide.

Condensation of various chlorides with piperidine derivatives such as 4-piperidone hydrochloride hydrate **13** or 1-Boc-4-piperidylmethanamine **15** yielded a series

of five piperidine analog amides in satisfactory yields (**Scheme 4; Table 2**).



**Scheme 4: Synthesis of piperidine amide derivatives.**

**Table 2: Synthesized products derived from piperidine with the amide bond studied.**

Compound ID	R	X	Yield
<b>14a</b>	H	O	72
<b>14b</b>	H	C=	63
<b>14c</b>	4-F	C=	58
<b>16a</b>	4-F	/	80
<b>16b</b>	H	/	87

The final structures of all the compounds synthesized have been established by the usual spectroscopic analyses, such as NMR and LC/MS, and the structures are in line with those expected.

#### Biological evaluation

The biological activity of each compound was evaluated on chloroquine-sensitive (3D7) and chloroquine-resistant (W2) *P. falciparum* strains, and the lethal dose on HUVEC cells was assessed.

**Table 3: *In vitro* antimalarial activity, cytotoxicity and selectivity index of compounds.**

Cpds ID	In vitro Activity ( $\mu\text{M} \pm \text{SD}$ )		HUVEC cells $\text{CC}_{50}$	Selectivity index : $\text{CC}_{50}/\text{IC}_{50}$	
	$\text{CI}_{50}$ (3D7)	$\text{CI}_{50}$ (W2)		(3D7)	(W2)
3a	72.45 $\pm$ 5.22	>100	88.23 $\pm$ 0.31	1.22	< 0.88
3b	>100	>100	>100	>1	>1
3c	33.65 $\pm$ 2.55	51.87 $\pm$ 3.04	>100	2.97	1.93
5a	>100	>100	89.74 $\pm$ 0.21	< 0.90	< 0.90
5b	>100	>100	84.67 $\pm$ 0.21	< 0.85	< 0.85
5c	>100	>100	>100	>1	>1
5d	>100	>100	>100	>1	>1
6	7.60 $\pm$ 1.30	40.25 $\pm$ 3.98	>100	> 13.16	> 2.48
8	1.36 $\pm$ 0.61	6.57 $\pm$ 1.24	85.78 $\pm$ 0.17	63.07	13.06
11	61.71 $\pm$ 1.60	>100	65.26 $\pm$ 0.52	1.06	< 0.65
12	6.12 $\pm$ 1.33	20.62 $\pm$ 2.67	92.73 $\pm$ 0.13	15.15	4.50
14a	>100	>100	>100	>1	>1
14b	>100	>100	73.34 $\pm$ 0.61	< 0.73	< 0.73
14c	/	/	/	/	/
16a	41.02 $\pm$ 2.20	33.25 $\pm$ 1.61	>100	> 2.44	> 3.01
16b	/	/	/	/	/
CQ	0,0156 $\pm$ 0,002	0,238 $\pm$ 0,019	>1	> 64.10	> 4.20

Based on Table 3, only seven compounds were active against the Pf3D7 strain and five against the PfW2 strain. Compound **8** showed the highest activity against both strains, with a  $\text{CI}_{50(3D7)}$  of 1.36  $\mu\text{M}$  and  $\text{CI}_{50(W2)}$  of 6.57  $\mu\text{M}$ , while compound **3a** was the least active ( $\text{CI}_{50} = 72.45 \mu\text{M}$ ). Compound **6** showed potent activity against the Pf3D7 strain, with an IC value of  $\text{IC}_{50} = 7.60 \mu\text{M}$ . There was no significant trend when assessing the effect of the substituent on the benzyl ring. On the other hand, it is

interesting to note the contribution of the 2-chlorobenzoyl group in the antiproliferative activity of malaria parasites (compared **6** and **8**). Among piperidine derivatives, only molecule **12** exhibited inhibitory potency on the susceptible strain, with a  $\text{CI}$  value $_{50}$  of 6.12  $\mu\text{M}$ . The introduction of cinnamoyl leading to **12** seems to play a crucial role in antiplasmodial activity (compared **11** and **12**).

Evaluation of the cytotoxic activity of all the compounds studied was relatively good, with a lethal dose ranging from 65.26  $\mu\text{M}$  to >100, confirming the safety of the compounds tested. Clearly, compound **8**, which showed the best activity, has the highest selectivity index, with a value of 63.

#### Analysis of drug similarity (ADME)

The success of a drug's journey through the human body is measured in the dimensions of Absorption, Distribution, Metabolism and Elimination (ADME).<sup>[23,24]</sup> Lipinski's Rule of Five (Ro5)<sup>[25,26]</sup> depends on four simple physicochemical parameter factors, which are: molecular weight not exceeding 500 g/mol, lipophilicity (Log P) less than 5, and a number of hydrogen bond acceptors and donors that should be less than 10 and 5,

respectively. Taking into account the *in vitro* assay, the drug properties of the compounds were evaluated according to ADMET parameters using the open offline server SwissADME (<http://www.swissadme.ch/>)<sup>[16]</sup> and the results are summarized in **Table 4**.

According to the *in silico* study, all the compounds synthesized meet Lipinski's Ro5 criteria. They have a molecular weight of between 274.32 and 475.41 g/mol, 1 to 4 hydrogen bond acceptors, and a hydrogen donor number of between 0 and 1. The log P partition coefficient, an important feature in the process of drug absorption and elimination, is between 1.98 and 5, in compliance with Ro5. No violation of Lipinski's Ro5 was observed for these compounds.

**Table 4: Drug similarity and Lipinski's rule of our ligands.**

Cpds ID	ABS	TPSA ( $\text{\AA}^2$ )	Molar refractivity	ROTB	MW	LogP	ALH	DLH	Lipinski violation	Log S	F
<b>Rule</b>	-	<140	40-130	$\leq 10$	< 500	$\leq 5$	< 10	< 5	< 2	$\leq 1$	>10%
3a	Haute	51,22	82,07	5	278,31	1,98	3	1	0	MS	0,55
3b	Haute	51,22	89,77	5	357,20	2,60	3	1	0	MS	0,55
3c	Haute	41,99	85,67	4	274,32	2,73	2	1	0	MS	0,55
5a	Haute	42,43	119,16	7	447,32	3,91	3	0	0	PS	0,55
5b	Haute	42,43	119,16	7	447,32	3,91	3	0	0	PS	0,55
5c	Haute	42,43	119,16	7	447,32	3,91	3	0	0	PS	0,55
5d	Haute	33,20	115,01	6	382,43	4,42	3	0	0	MS	0,55
6	Haute	24,92	83,24	3	313,19	3,50	1	1	0	MS	0,55
8	Haute	33,20	118,06	5	451,74	5,03	2	0	0	PS	0,55
11	Haute	41,57	95,44	5	345,26	3,47	2	1	0	MS	0,55
12	Haute	49,85	134,96	8	475,41	4,58	3	0	0	PS	0,55
16a	Haute	58,64	103,59	8	362,44	2,91	4	1	0	MS	0,55

**ABS:** absorption. **TPSA:** Topological Polar Surface Area. **HBA:** H-bond acceptor. **HBD:** H-bond donor **n-ROTB:** Number of rotatable bonds. **MW:** Molecular weight. **LogP:** logarithm of partition coefficient of compound between n-octanol and water. **F:** Bioavailability Score. **MS:** Moderately soluble. **PS:** Poorly soluble.

In addition, topological polar area (TPSA) values of less than 140  $\text{\AA}^2$  indicate good permeability through the cell plasma membrane.<sup>[27]</sup> In addition, the number of flexible bonds is between 4 and 8, which does not adversely affect the permeation rate. As with the absorption of the molecule in the gut, all compounds show high gastrointestinal absorption, indicating that they are highly absorbed in the gut.

The results of this study show that the compounds meet the criteria established by ADMET, suggesting that they can be administered orally. Furthermore, when comparing *in vitro* and *in silico* results, compound **8** stands out for its potential promise in terms of pharmacological properties, making it a promising prototype.

#### Molecular docking

G9a, also known as Euchromatin Histone Lysine Methyl Transferase 2 (EHMT2), is an enzyme that catalyzes the addition of methyl groups to histone H3 lysine 9.<sup>[28-30]</sup> This epigenetic modification plays a crucial role in many

biological processes. Because of the importance of G9a, several inhibitors of this enzyme have been developed.<sup>[29,30]</sup> Competitive SAM inhibitors bind to the SAM cofactor binding pocket of G9a, thus preventing histone methylation and, consequently, reducing the enzymatic activity of G9a. These inhibitors offer a promising strategy for disrupting G9a-dependent gene regulatory pathways.

It's worth noting that histone lysine methyltransferases (HKMTs) are present not only in mammalian systems, but also in *P. falciparum*, one of the agents responsible for human malaria. In the case of the parasite, these proteins play an essential role in regulating the gene transcription pathway. Therefore, by specifically targeting G9a, it is possible to disrupt these processes in *P. falciparum*. To further investigate competitive inhibitors of G9a, we have chosen the human G9a receptor (PDB ID:2O8J) as the anchor for our structures. This will enable us to explore competitive inhibitors specific to the EHMT2 substrate.

To explore ligand binding sites on the structure of the receptor enzyme EHMT2, its 3D structure was downloaded from RCSB-PDB ([www.rcsb.org/pdb](http://www.rcsb.org/pdb)). Ligands and receptor were prepared for docking by minimizing their energy, followed by 3D protonation in MOE 2015.10<sup>[31]</sup> eliminating water molecules on G9a, facilitating the interaction of ligands with the receptor.<sup>[18,32]</sup> MOE uses an empirical swimming function (GBVI/WSA dG), based on the force field, to calculate binding affinity.<sup>[11]</sup>

**Table 5: S-score binding energy values of selected synthesized ligands.**

N <sup>o</sup>	Ligand name	S value (Kcal/mol)
1	5a	-7.3805
2	5b	-7.2362
3	5c	-7.4593
4	6	-6.4672
5	8	-7.1898
6	12	-7.3911
7	CQ	-6.8021

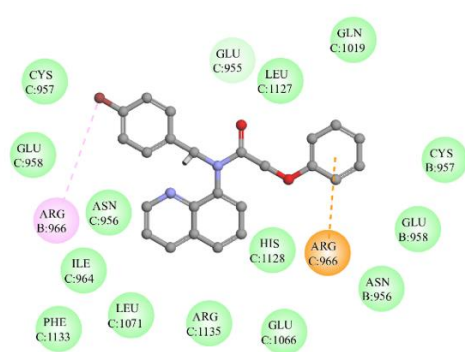
The energy values generated by the MOE-Dock software (**Table 5**) showed that the selected compounds had the lowest binding energy values, ranging from **-7.46** to **-6.47** kcal/mol among the compounds tested. All molecules showed a high affinity for G9a.

Similar to *in silico* docking, ligand **5c** showed a minimum energy of **-7.46** kcal/mol, making it the

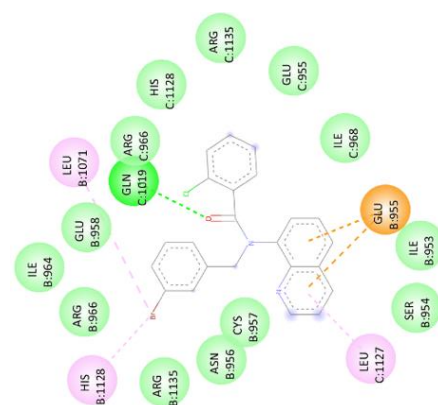
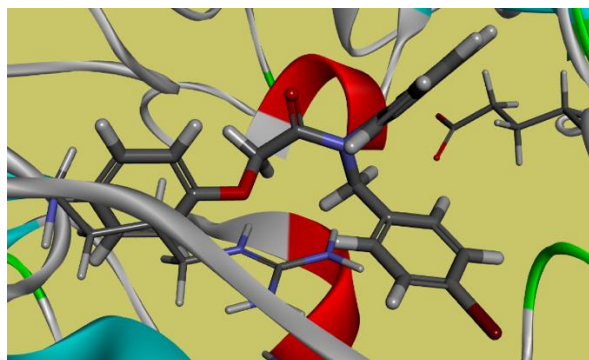
strongest interaction to inhibit G9a activity. However, *in vitro*, it showed no biological activity ( $IC_{50} > 100$ ). Compound **12** showed the second highest affinity with the EHMT2 target, exhibiting a lower binding energy than chloroquine, with a value of **-7.39** kcal/mol versus **-6.80** kcal/mol. The analog *N*-[3-bromobenzyl]-2-chloro-*N*-(8-quinolyl)benzamide **8** satisfies all the parameters of Lipinski's rule, showing a minimum energy of **-7.19** kcal/mol, making it a potentially orally active drug.

Analysis of the pharmacophore map of compound **8** with EHMT2 revealed a significant interaction in the form of a hydrogen bond between the oxygen of the amide function and residue GLN1019 of the enzyme's C-chain active site. In addition to this hydrogen bond, pi-anion and pi-alkyl interactions were observed (**fig. 2**). Similarly, compound **12** also showed a significant interaction with G9a. A hydrogen bond was formed between this compound and ARG residue B:966, in addition to electrostatic and hydrophobic interactions (**fig. 3**). These results support the hypothesis that compounds **8** and **12** possess potentially strong biological activity in blocking the growth of *P. falciparum* parasites through their interaction with G9a.

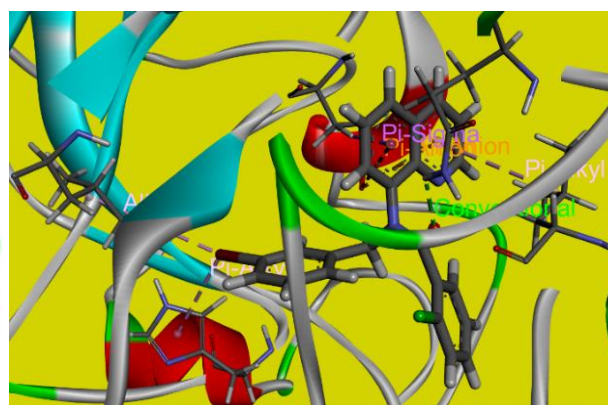
The intermolecular interactions between the compounds and the G9a target (ID:2O8J) were visualized using Discovery Studio Visualizer software, providing insight into the molecular mechanisms underlying the compounds' activity.



**Figure 1: 2D and 3D image of interactions between G9a active site residues and compound 5c.**



**Figure 2: 2D and 3D image of interactions between G9a active site residues and compound 8.**



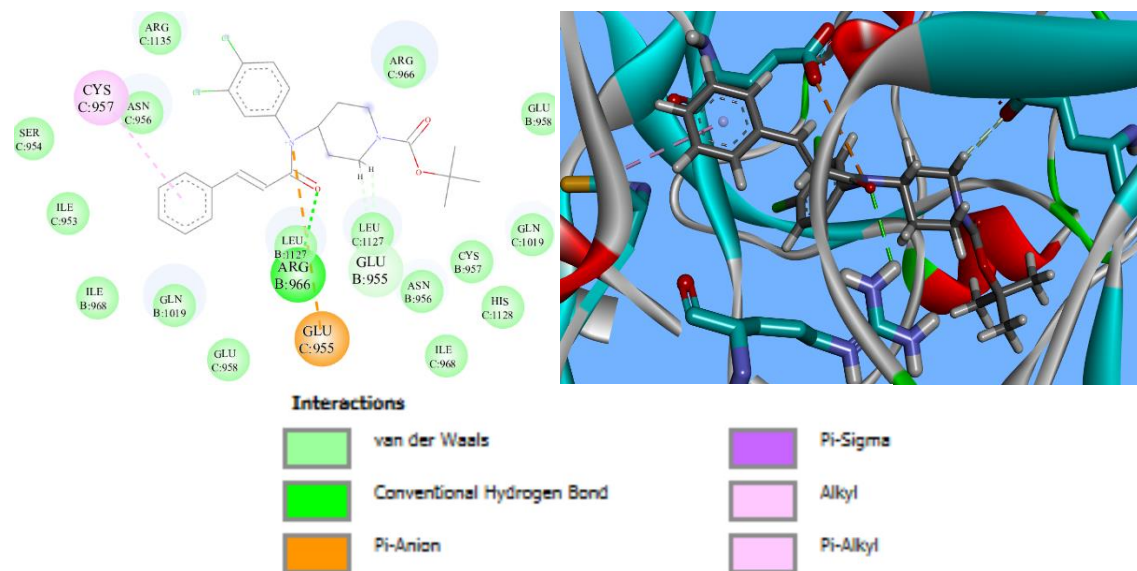


Figure 3: 2D and 3D image of interactions between G9a active site residues and compound 12.

### Characteristics of Synthetic Molecules

#### 2-phenoxy-*N*-(quinolin-8-yl)acetamide (3a)

Yield: 99%; MS: (ESI, +) for  $C_{17}H_{14}N_2O_2$  [M+H]<sup>+</sup> calculated 278.1055 m/z, found 279.1154 m/z; <sup>1</sup>H NMR (300 MHz, CDCl<sub>3</sub>) δ 10.98 (s, 1H, NH), 8.86 (dd, *J* = 9.0, 4.9 Hz, 2H, 2CH<sub>Ar</sub>), 8.17 (dd, *J* = 8.3, 1.7 Hz, 1H, CH), 7.62 - 7.52 (m, 2H, 2CH<sub>Ar</sub>), 7.47 (dd, *J* = 8.3, 4.2 Hz, 1H), 7.38 (t, *J* = 15.1, 6.1 Hz, 2H, 2CH), 7.21 - 7.12 (m, 2H), 7.07 (t, *J* = 7.3 Hz, 1H), 4.77 (s, 2H, CH<sub>2</sub> O). <sup>13</sup>C NMR (75 MHz, CDCl<sub>3</sub>) δ 166.83 (C=O), 157.44 (C-OAr), 148.66 (C=NAr), 138.80, 136.20, 133.74, 129.79 (2CH<sub>Ar</sub>), 128.00, 127.23, 122.24 (2CH<sub>Ar</sub>), 121.72, 116.80, 115.16 (2CH<sub>Ar</sub>), 68.16 (CH<sub>2</sub>).

#### 2-(4-bromophenoxy)-*N*-(8-quinolyl)acetamide (3b)

Yield: 90%; MS: (ESI, +) for  $C_{13}H_{17}BrN_2O_2$  [M+H]<sup>+</sup> calculated 356.0160 m/z, found 357.0244 m/z; <sup>1</sup>H NMR (300 MHz, Chloroform-*d*) δ 10.90 (s, 1H), 8.91 - 8.75 (m, 2H), 8.24 - 8.13 (m, 1H), 7.65 - 7.41 (m, 6H), 7.09 - 6.96 (m, 2H), 4.74 (s, 1H).

#### (2*E*)-3-phenyl-*N*-(8-quinolyl)prop-2-enamide (3c)

Yield: 88%; MS: (ESI, +) for  $C_{18}H_{14}N_2$  [M+H]<sup>+</sup> calculated 274.1106 m/z, found 275.1186 m/z; <sup>1</sup>H NMR (300 MHz, Chloroform-*d*) δ 10.03 (s, 1H, NH), 8.94 (dd, *J* = 7.4, 1.7 Hz, 1H), 8.86 (dd, *J* = 4.2, 1.7 Hz, 1H), 8.20 (dd, *J* = 8.3, 1.7 Hz, 1H), 7.85 (d, *J* = 15.6 Hz, 1H), 7.64 (dq, *J* = 6.7, 2.5 Hz, 2H), 7.61 - 7.52 (m, 2H), 7.52 - 7.42 (m, 2H), 7.42 - 7.34 (m, 2H), 6.83 (d, *J* = 15.6 Hz, 1H). <sup>13</sup>C NMR (75 MHz, Chloroform-*d*) δ 164.13 (C=O), 148.15, 142.09, 138.51, 136.42, 134.86, 134.68, 129.89, 128.87 (2CH<sub>Ar</sub>), 128.04 (2CH<sub>Ar</sub>), 128.00, 127.51, 121.65, 121.61, 117.37-116.53 (4CH).

#### *N*-(2-bromobenzyl)-2-phenoxy-*N*-(8-quinolyl)acetamide (5a)

Yield: 69%; MS: (ESI, +) for  $C_{24}H_{19}BrN_2O_2$  [M+3H]<sup>+</sup> calculated 446.0630 m/z, found 449.0713 m/z; <sup>1</sup>H NMR (300 MHz, CDCl<sub>3</sub>) δ 8.78 (dd, *J* =

4.2, 1.7 Hz, 1H), 8.11 (dd, *J* = 8.3, 1.7 Hz, 1H), 7.69 - 7.55 (m, 3H), 7.50 - 7.30 (m, 4H), 7.28 - 7.08 (m, 4H), 6.75 (s, 1H), 6.59 (dd, *J* = 7.7, 1.1 Hz, 1H), 4.75 (s, 2H), 4.67 (d, *J* = 5.5 Hz, 2H). <sup>13</sup>C NMR (75 MHz, DMSO-*d*<sub>6</sub>) δ 164.20, 155.04, 148.77, 147.33, 142.46, 139.82, 138.99, 131.81, 131.69, 127.90, 127.77, 127.00, 123.98, 121.49, 118.11, 117.47, 114.82, 114.54, 112.78, 112.47, 101.74, 56.04.

#### *N*-(3-bromobenzyl)-2-phenoxy-*N*-(8-quinolyl)acetamide (5b)

Yield: 60%; MS: (ESI, +) for  $C_{24}H_{19}BrN_2O_2$  [M+3H]<sup>+</sup> calculated 446.0630 m/z, found 449.0713 m/z; <sup>1</sup>H NMR (300 MHz, CDCl<sub>3</sub>) δ 9.03 (dd, *J* = 4.2, 1.7 Hz, 1H), 8.25 (dd, *J* = 8.3, 1.7 Hz, 1H), 7.87 (dd, *J* = 8.3, 1.4 Hz, 1H), 7.59 - 7.41 (m, 2H), 7.44 (s, 1H), 7.36 (d, *J* = 7.7 Hz, 1H), 7.31 - 7.04 (m, 5H), 6.92 (t, *J* = 9.0, 6.0 Hz, 1H), 6.77 (d, *J* = 7.9 Hz, 2H), 5.72 (s, 2H, CH<sub>2</sub>N), 4.33 (s, 2H, CH<sub>2</sub>O). <sup>13</sup>C NMR (75 MHz, CDCl<sub>3</sub>) δ 168.99, 158.01, 151.25, 144.11, 139.84, 137.63, 136.48, 131.98, 130.48, 129.83, 129.61, 129.55, 129.27 (2CH<sub>Ar</sub>), 129.09, 127.66, 126.29, 122.31, 122.22, 121.15, 114.63 (2CH<sub>Ar</sub>), 66.63 (CH<sub>2</sub>O), 52.76 (CH<sub>2</sub>N).

#### *N*-(4-bromobenzyl)-2-phenoxy-*N*-(8-quinolyl)acetamide (5c)

Yield: 40%; MS: (ESI, +) for  $C_{24}H_{19}BrN_2O_2$  [M+3H]<sup>+</sup> calculated 446.0630 m/z, found 449.0687 m/z; <sup>1</sup>H NMR (300 MHz, CDCl<sub>3</sub>) δ 8.93 (dd, *J* = 4.2, 1.7 Hz, 1H), 8.15 (dd, *J* = 8.3, 1.8 Hz, 1H), 7.77 (dd, *J* = 8.3, 1.4 Hz, 1H), 7.44 (dd, *J* = 8.3, 4.2 Hz, 1H), 7.36 (dd, *J* = 8.3, 7.3 Hz, 1H), 7.31 - 7.21 (m, 2H), 7.11 (td, *J* = 8.3, 2.1 Hz, 3H), 7.06 - 6.96 (m, 2H), 6.83 (t, *J* = 7.3 Hz, 1H), 6.66 (d, 2H), 5.64 (s, 2H), 4.31 (s, 2H).

<sup>13</sup>C NMR (75 MHz, CDCl<sub>3</sub>) δ 168.91 (C=O), 158.01, 151.27, 144.12, 137.59, 136.59, 136.47, 131.38

(2CHAr), 130.91, 129.60 (2CHAr), 129.24 (2CHAr), 129.04, 126.26, 122.21, 121.39, 121.14, 114.63 (2CHAr), 66.61 (CH<sub>2</sub>O), 52.60 (CH<sub>2</sub>N).

**(2E)-N-(2-bromobenzyl)-3-phenyl-N-(8-quinolyl)prop-2-enamide (5d)**

Yield: 75%; MS: (ESI, +) for C<sub>25</sub>H<sub>19</sub>FN<sub>2</sub>O [M+H]<sup>+</sup> calculated 382.1481 m/z, found 383.1605 m/z; <sup>1</sup>H NMR (300 MHz, CDCl<sub>3</sub>) δ 9.00 (dd, *J* = 4.2, 1.8 Hz, 1H), 8.25 (dd, *J* = 8.3, 1.8 Hz, 1H), 7.87 (dd, *J* = 8.3, 1.4 Hz, 1H), 7.77 (d, *J* = 15.5 Hz, 1H), 7.56 – 7.39 (m, 3H), 7.32 – 7.10 (m, 6H), 6.99 – 6.83 (m, 2H), 6.11 (d, *J* = 15.6 Hz, 1H), 5.91 (d, *J* = 14.4 Hz, 1H), 5.31 (s, 2H).

<sup>13</sup>C NMR (75 MHz, CDCl<sub>3</sub>) δ 166.83, 162.07 (d, *J* = 245.0 Hz, CF), 151.07, 144.49, 142.03, 138.70, 136.30, 135.28, 133.89, 130.85, 130.74, 130.62, 129.50, 129.31, 128.59, 128.51, 127.73, 126.07, 121.99, 119.18, 115.12, 114.84, 52.09.

**N-[(3-bromobenzyl)quinolin-8-amine (6)**

Yield: 69%; MS: (ESI, +) for C<sub>16</sub>H<sub>13</sub>BrN<sub>2</sub> [M+2H]<sup>+</sup> calculated 313.0262 m/z, found 315.0320 m/z; <sup>1</sup>H NMR (300 MHz, CDCl<sub>3</sub>) δ 8.76 (dd, *J* = 4.2, 1.7 Hz, 1H), 8.10 (dd, *J* = 8.3, 1.7 Hz, 1H), 7.62 (d, *J* = 1.9 Hz, 1H), 7.48 – 7.29 (m, 4H), 7.22 (t, *J* = 7.8 Hz, 1H), 7.10 (dd, *J* = 8.2, 1.2 Hz, 1H), 6.67 (s, 1H), 6.62 (dd, *J* = 7.6, 1.2 Hz, 1H), 4.57 (d, *J* = 5.9 Hz, 2H). <sup>13</sup>C NMR (75 MHz, CDCl<sub>3</sub>) δ 147.03, 144.27 (C<sup>IV</sup>), 141.86 (C<sup>IV</sup>), 138.24 (C<sup>IV</sup>), 136.06 (CH), 130.30, 130.26, 130.18, 128.66, 127.69, 125.82, 122.79 (C<sup>IV</sup>), 121.48, 114.55, 105.25, 47.20.

**N-(3-bromobenzyl)-2-chloro-N-(8-quinolyl)benzamide (8)**

Yield: 72%; MS: (ESI, +) for C<sub>23</sub>H<sub>16</sub>BrClN<sub>2</sub>O [M+2H]<sup>+</sup> calculated 451.0135 m/z, found 453.0229 m/z; <sup>1</sup>H NMR (300 MHz, CDCl<sub>3</sub>) δ 9.07 (dd, *J* = 4.2, 1.7 Hz, 1H), 8.09 (dd, *J* = 8.3, 1.7 Hz, 1H), 7.60 (dd, *J* = 8.2, 1.4 Hz, 1H), 7.53 (d, *J* = 1.9 Hz, 1H), 7.47 (dd, *J* = 8.3, 4.2 Hz, 1H), 7.41 – 7.25 (m, 3H), 7.22 – 7.07 (m, 2H), 7.01 (dd, *J* = 7.7, 1.7 Hz, 1H), 6.93 (td, *J* = 7.8, 1.7 Hz, 1H), 6.68 (td, *J* = 7.5, 1.1 Hz, 1H), 6.11 (d, *J* = 14.8 Hz, 1H), 4.52 (d, *J* = 14.8 Hz, 2H). <sup>13</sup>C NMR (75 MHz, CDCl<sub>3</sub>) δ 168.80, 150.75, 143.94, 139.91, 138.11, 136.54, 136.35, 131.81, 130.71, 130.39, 129.91, 129.76, 129.62, 129.09, 129.02, 128.72, 127.45, 127.20, 125.85, 125.73, 122.31, 121.81, 51.73.

**1-Boc-4-(3,4-dichloroanilino)piperidine (11)**

Yield: 68%; MS: (ESI, +) for C<sub>16</sub>H<sub>22</sub>Cl<sub>2</sub>N<sub>2</sub>O<sub>2</sub> [M+H]<sup>+</sup> calculated 344.1058 m/z, found 445.1164 m/z; <sup>1</sup>H NMR (300 MHz, Chloroform-*d*) δ 7.10 (d, *J* = 8.7 Hz, 1H), 6.58 (d, *J* = 2.8 Hz, 1H), 6.34 (dd, *J* = 8.7, 2.8 Hz, 1H), 3.97 (d, *J* = 13.6 Hz, 2H), 3.54 (s, 1H), 3.35 – 3.21 (m, 2H), 2.85 (q, *J* = 14.0, 11.4, 2.8 Hz, 1H), 1.99 – 1.87 (m, 2H), 1.39 (s, 9H), 1.36 – 1.16 (m, 2H). <sup>13</sup>C NMR (75 MHz, CDCl<sub>3</sub>) δ 146.28, 132.95, 130.70, 119.85, 114.15, 112.96, 79.73 (C<sup>IV</sup>), 50.22 (2CH<sub>2</sub>), 42.54, 32.14 (2CH<sub>2</sub>), 28.42 (3CH<sub>3</sub>).

***t*-butyl 4-(3,4-dichloro-N-[(E)-3-phenylprop-2-enyl]anilino)piperidine-1-carboxylate (12)**

Yield: 28%; MS: (ESI, +) for C<sub>25</sub>H<sub>28</sub>Cl<sub>2</sub>N<sub>2</sub>O<sub>3</sub> [M+H]<sup>+</sup> calculated 474.1477 m/z, found 475.0247 m/z; <sup>1</sup>H NMR (300 MHz, CDCl<sub>3</sub>) δ 7.62 (d, *J* = 15.4 Hz, 1H), 7.46 (d, *J* = 8.5 Hz, 1H), 7.21 (d, *J* = 13.0 Hz, 6H), 6.93 (dd, *J* = 8.4, 2.4 Hz, 1H), 5.98 (d, *J* = 15.4 Hz, 1H), 4.80 (d, *J* = 11.9 Hz, 1H), 4.10 (d, *J* = 13.3 Hz, 2H), 3.32 (q, *J* = 7.0 Hz, 2H), 1.94 – 1.58 (m, 4H), 1.35 (s, 9H).

**1-(2-phenoxyacetyl)piperidin-4-one (14a)**

Yield: 72%; MS: (ESI, +) for C<sub>13</sub>H<sub>15</sub>NO<sub>3</sub> [M+H]<sup>+</sup> calculated 233.1052 m/z, found 234.1131 m/z; <sup>1</sup>H NMR (300 MHz, CDCl<sub>3</sub>) δ 7.39 – 7.25 (m, 2H, 2CH), 7.09 – 6.92 (m, 3H, 3CH), 4.79 (d, *J* = 1.5 Hz, 2H, CH<sub>2</sub>), 3.90 (t, *J* = 6.3 Hz, 4H, 2CH<sub>2</sub>), 2.49 (q, *J* = 6.7 Hz, 4H, 2CH<sub>2</sub>). <sup>13</sup>C NMR (75 MHz, CDCl<sub>3</sub>) δ 206.26 (C=O), 166.99 (NC=O), 157.66 (C<sup>IV</sup>), 129.77 (2CH), 121.96 (CH), 114.46 (2CH), 68.03 (CH<sub>2</sub>O), 44.08 (2CH<sub>2</sub>N), 41.51 (2CH<sub>2</sub>).

**1-[(E)-3-phenylprop-2-enyl]piperidin-4-one (14b)**

Yield: 63%; MS: (ESI, +) for C<sub>14</sub>H<sub>15</sub>NO<sub>2</sub> [M+H]<sup>+</sup> calculated 229.1103 m/z, found 230.1174 m/z; <sup>1</sup>H NMR (300 MHz, CDCl<sub>3</sub>) δ 7.77 (d, *J* = 15.5 Hz, 1H), 7.66 – 7.49 (m, 4H), 7.41 (dd, *J* = 7.4, 2.8 Hz, 1H), 6.96 (dd, *J* = 15.4, 2.5 Hz, 1H), 3.99 (d, *J* = 7.9 Hz, 4H), 2.57 (dd, *J* = 7.5, 5.0 Hz, 4H). <sup>13</sup>C NMR (75 MHz, MD<sub>3</sub>OD) δ 207.76 (C=O), 166.31 (NC=O), 143.29 (CH), 135.13 (C<sup>IV</sup>), 129.59 (CH<sup>Ar</sup>), 128.47 (2CH<sup>Ar</sup>), 127.55 (2CH<sup>Ar</sup>), 117.09 (CH), 39.58 (2CH<sub>2</sub>), 34.80 (2CH<sub>2</sub>).

**1-[(E)-3-(4-fluorophenyl)prop-2-enyl]piperidin-4-one (14c)**

Yield: 58%; MS: (ESI, +) for C<sub>14</sub>H<sub>14</sub>NFO<sub>2</sub> [M+H]<sup>+</sup> calculated 247.1009 m/z, found 248.1247 m/z; <sup>1</sup>H NMR (300 MHz, CDCl<sub>3</sub>) δ 7.77 (d, *J* = 15.3 Hz, 1H), 7.66 – 7.49 (m, 2H), 7.41 (dd, *J* = 7.4, 3.2 Hz, 2H), 6.98 (dd, *J* = 14.9, 2.5 Hz, 1H), 3.89 (d, *J* = 8.3 Hz, 4H), 2.67 (dd, *J* = 7.5, 5.0 Hz, 4H). <sup>13</sup>C NMR (75 MHz, MD<sub>3</sub>OD) δ 207.56 (C=O), 166.38 (NC=O), 161.80 (CF), 134.23 (C<sup>IV</sup>), 130.59 (CH), 129.47 (2CH<sup>Ar</sup>), 125.5 (2CH<sup>Ar</sup>), 118.49 (CH), 40.58 (2CH<sub>2</sub>), 34.70 (2CH<sub>2</sub>).

***t*-butyl 4-[(E)-4-fluorocinnamoyl]aminomethyl]piperidine-1-carboxylate (16a)**

Yield: 80%; MS: (ESI, +) for C<sub>20</sub>H<sub>27</sub>FN<sub>2</sub>O<sub>3</sub>.H<sub>2</sub>O [M+5H]<sup>+</sup> calculated 380.2111 m/z, found 385.1900 m/z; <sup>1</sup>H NMR (300 MHz, CDCl<sub>3</sub>) δ 7.61 (d, *J* = 15.6 Hz, 1H), 7.49 (dd, *J* = 8.3, 5.6 Hz, 2H), 7.15 – 7.01 (m, 2H), 6.33 (d, *J* = 15.5 Hz, 1H), 5.83 (s, 1H), 4.22 – 4.05 (m, 2H), 3.31 (s, 2H), 2.71 (t, *J* = 12.7 Hz, 2H), 2.10 (m, 1H), 2.08 (dd, *J* = 13.2, 1.2 Hz, 4H), 1.28 (s, 9H).

***t*-butyl 4-[(E)-cinnamoyl]aminomethyl]piperidine-1-carboxylate (16b)**

Yield: 65%; MS: (ESI, +) for C<sub>20</sub>H<sub>28</sub>N<sub>2</sub>O<sub>3</sub> [M+H]<sup>+</sup> calculated 344.2100 m/z, found 345.2308 m/z; <sup>1</sup>H NMR (300 MHz, CDCl<sub>3</sub>) δ 7.58 (dd, *J* = 9.7, 5.3

Hz, 2H), 7.53 (d,  $J = 15.4$  Hz, 1H), 7.41 – 7.37 (m, 3H), 6.55 (d,  $J = 15.2$  Hz, 1H), 5.83 (s, 1H), 3.68 (dt,  $J = 12.4, 7.0$  Hz, 2H), 3.41 (dt,  $J = 12.4, 7.1$  Hz, 2H), 3.18 (d,  $J = 9.2$  Hz, 2H), 1.89 – 1.80 (m, 4H), 1.75 (m, 1H), 1.46 (s, 9H).

## CONCLUSION

This multidisciplinary study combines the synthesis of quinoline and piperidine derivatives, *in vitro* methods to assess antimalarial and cytotoxic activity, and *in silico* molecular modeling. Compounds **8** and **12** showed interesting properties against Pf3D7 and PfW2 strains. The predictive ADME properties identified promising compounds that could be potential therapeutic agents in drug discovery and development. Compounds **8** and **12** can also be used to develop orally active drugs for the treatment of malaria. This study provides a clearer insight into the interaction properties of synthetic inhibitors with the EHMT2 protein. The results obtained could contribute to the development of new, more effective, safe and targeted antimalarial drugs, paving the way for new strategies in the fight against malaria.

## ACKNOWLEDGMENTS

We would like to express our deep gratitude to the Senegalese government. We would also like to thank the French Cooperation for having made this thesis work possible by granting a 12-month scholarship. We are also grateful to the BioCIS laboratory at the Université Paris-Saclay for their invaluable collaboration. Their expertise and access to state-of-the-art equipment, notably for bioactive assays, LC/MS and NMR analysis, greatly contributed to the success of this study.

## REFERENCES

1. WHO. WHO Guidelines for Malaria - 3 June 2022||Targeted Testing and Treatment (TTaT). Geneva: World Health Organization, 2022; 2022: 396.
2. Taylor, H. M.; Triglia, T.; Thompson, J.; Sajid, M.; Fowler, R.; Wickham, M. E.; Cowman, A. F.; Holder, A. A. Plasmodium Falciparum Homologue of the Genes for Plasmodium Vivax and Plasmodium yoelii Adhesive Proteins, Which Is Transcribed but Not Translated. *Infect. Immun.*, 2001; 69(6).
3. Dondorp, A. M.; Nosten, F.; Yi, P.; Das, D.; Phyto, A. P.; Tarning, J.; Lwin, K. M.; Ariey, F.; Hanpithakpong, W.; Lee, S. J.; Ringwald, P.; Silamut, K.; Imwong, M.; Chotivanich, K.; Lim, P.; Herdman, T.; An, S. S.; Yeung, S.; Singhasivanon, P.; Day, N. P. J.; Lindegardh, N.; Socheat, D.; White, N. J. Artemisinin Resistance in Plasmodium Falciparum Malaria. *N. Engl. J. Med.*, 2009; 361(5): 455–467.
4. Noedl, H.; Socheat, D.; Satimai, W. Artemisinin-Resistant Malaria in Asia. *N. Engl. J. Med.*, 2009; 361(5): 540–541.
5. Gogtay, N.; Kannan, S.; Thatte, U. M.; Olliaro, P. L.; Sinclair, D. Artemisinin-Based Combination Therapy for Treating Uncomplicated Plasmodium Vivax Malaria. *Cochrane Database Syst. Rev.*, 2013; 2013(10): CD008492.
6. Flannery, E. L.; Chatterjee, A. K.; Winzeler, E. A. Antimalarial Drug Discovery - Approaches and Progress towards New Medicines. *Nat. Rev. Microbiol.*, 2013; 11(12): 849–862.
7. Burrows, J. N.; Hooft van Huijsduijnen, R.; Möhrle, J. J.; Oeuvray, C.; Wells, T. N. Designing the next Generation of Medicines for Malaria Control and Eradication. *Malar. J.*, 2013; 12(1): 187.
8. Van de Walle, T.; Cools, L.; Mangelinckx, S.; D'hooghe, M. Recent Contributions of Quinolines to Antimalarial and Anticancer Drug Discovery Research. *Eur. J. Med. Chem.*, 2021; 226: 113865.
9. Dolezal, M.; Palek, L.; Vinsova, J.; Buchta, V.; Jampilek, J.; Kralova, K. Substituted Pyrazinecarboxamides: Synthesis and Biological Evaluation. *Molecules*, 2006; 11(4): 242–256.
10. Tiglani, D.; Salahuddin; Mazumder, A.; Yar, M. S.; Kumar, R.; Ahsan, M. J. Benzimidazole-Quinoline Hybrid Scaffold as Promising Pharmacological Agents: A Review. *Polycycl. Aromat. Compd.*, 2022; 42(8): 5044–5066.
11. Attique, S. A.; Hassan, M.; Usman, M.; Atif, R. M.; Mahboob, S.; Al-Ghanim, K. A.; Bilal, M.; Nawaz, M. Z. A Molecular Docking Approach to Evaluate the Pharmacological Properties of Natural and Synthetic Treatment Candidates for Use against Hypertension. *Int. J. Environ. Res. Public Health*, 2019; 16(6): 923.
12. Manga, A.; Gassama, A.; Diatta, K.; Bassène, E.; Cojean, S.; Cavé, C. Antiplasmodial Activity of Extracts of Khaya Senegalensis (Ders.) A. Jus (Meliaceae) and Melia Azedarach L., Plants of Senegalese Traditional Medicine, 2018.
13. Smilkstein, M.; Sriwilaijaroen, N.; Kelly, J. X.; Wilairat, P.; Riscoe, M. Simple and Inexpensive Fluorescence-Based Technique for High-Throughput Antimalarial Drug Screening. *Antimicrob. Agents Chemother.*, 2004; 48(5): 1803–1806.
14. Johnson, J. D.; Dennon, R. A.; Gerena, L.; Lopez-Sanchez, M.; Roncal, N. E.; Eaux, N. C. Assessment and Continued Validation of the Malaria SYBR Green I-Based Fluorescence Assay for Use in Malaria Drug Screening. *Antimicrob. Agents Chemother.*, 2007; 51(6): 1926–1933.
15. GLACE. Introduction à la méthode. <http://www.antimalarial-icestimator.net/MethodIntro.htm> (accessed 2023-09-05).
16. Daina, A.; Michielin, O.; Zoete, V. SwissADME: A Free Web Tool to Evaluate Pharmacokinetics, Drug-Likeness and Medicinal Chemistry Friendliness of Small Molecules. *Sci. Rep.*, 2017; 7(1): 42717.
17. Wu, H.; Min, J.; Lunin, V. V.; Antoshenko, T.; Dombrovski, L.; Zeng, H.; Allali-Hassani, A.;

- Campagna-Slater, V.; Vedadi, M.; Arrowsmith, C. H.; Plotnikov, A. N.; Schapira, M. Structural Biology of Human H3K9 Methyltransferases. *PLoS One*, 2010; 5(1): e8570.
18. Clark, A. M.; Labute, P. 2D Depiction of Protein–Ligand Complexes. *J. Chem. Inf. Model.*, 2007; 47(5): 1933–1944.
19. Inc, C. C. G. Molecular Operating Environment (MOE). *Chem. Comput. Group Inc*, 2016; 1010.
20. Carlsen, L.; Dopp, D.; Dopp, H.; Duus, F.; Hartmann, H.; Lang-Fugmann, S.; Schulze, B.; Smalley, R. K.; Wakefield, B. J. Houben-Weyl Methods in Organic Chemistry, 1992.
21. Khan, S. N.; Bae, S.-Y.; Kim, H.-S. A Highly Stereoselective Reductive Amination of 3-Ketosteroid with Amines: An Improved Synthesis of 3 $\alpha$ -Aminosteroid. *Tetrahedron Lett.*, 2005; 46(45): 7675–7678.
22. Boros, E. E.; Thompson, J. B.; Katamreddy, S. R.; Carpenter, A. J. Facile Reductive Amination of Aldehydes with Electron-Deficient Anilines by Acyloxyborohydrides in TFA: Application to a Diazaindoline Scale-Up. *J. Org. Chem.*, 2009; 74(9): 3587–3590.
23. Hospital, A.; Goñi, J. R.; Orozco, M.; Gelpí, J. L. Molecular Dynamics Simulations: Advances and Applications. *Adv. Appl. Bioinforma. Chem.*, 2015; 8: 37–47.
24. Freire, A. C.; Podczek, F.; Sousa, J.; Veiga, F. Liberação específica de fármacos para administração no cólon por via oral. I - O cólon como local de liberação de fármacos. *Rev. Bras. Ciênc. Farm.*, 2006; 42: 319–335.
25. Lipinski, C. A.; Lombardo, F.; Dominy, B. W.; Feeney, P. J. Experimental and Computational Approaches to Estimate Solubility and Permeability in Drug Discovery and Development Settings. *Adv. Drug Deliv. Rev.*, 2001; 46(1–3): 3–26.
26. Fidelis Toloyi Ndombera; Geoffrey K. K. Maiyoh; Vivian C. Tuei. Pharmacokinetic, Physicochemical and Medicinal Properties of N-Glycoside Anti-Cancer Agent More Potent than 2-Deoxy-D-Glucose in Lung Cancer Cells. *J. Pharm. Pharmacol.*, 2019; 7(4).
27. Veber, D. F.; Johnson, S. R.; Cheng, H.-Y.; Smith, B. R.; Ward, K. W.; Kopple, K. D. Molecular Properties That Influence the Oral Bioavailability of Drug Candidates. *J. Med. Chem.*, 2002; 45(12): 2615–2623.
28. Ding, J.; Li, T.; Wang, X.; Zhao, E.; Choi, J.-H.; Yang, L.; Zha, Y.; Dong, Z.; Huang, S.; Asara, J. M.; Cui, H.; Ding, H.-F. The Histone H3 Methyltransferase G9A Epigenetically Activates the Serine-Glycine Synthesis Pathway to Sustain Cancer Cell Survival and Proliferation. *Cell Metab.*, 2013; 18(6): 896–907.
29. Wood, A.; Shilatifard, A. Posttranslational Modifications of Histones by Methylation. *Adv. Protein Chem.*, 2004; 67: 201–222.
30. Branscombe, T. L.; Frankel, A.; Lee, J. H.; Cook, J. R.; Yang, Z.; Pestka, S.; Clarke, S. PRMT5 (Janus Kinase-Binding Protein 1) Catalyzes the Formation of Symmetric Dimethylarginine Residues in Proteins. *J. Biol. Chem.*, 2001; 276 (35): 32971–32976.
31. Scholz, C.; Knorr, S.; Hamacher, K.; Schmidt, B. DOCKTITE—A Highly Versatile Step-by-Step Workflow for Covalent Docking and Virtual Screening in the Molecular Operating Environment. *J. Chem. Inf. Model.*, 2015; 55(2): 398–406.
32. Laleu, B.; Akao, Y.; Ochida, A.; Duffy, S.; Lucantoni, L.; Shackelford, D. M.; Chen, G.; Katneni, K.; Chiu, F. C. K.; White, K. L.; Chen, X.; Sturm, A.; Dechering, K. J.; Crespo, B.; Sanz, L. M.; Wang, B.; Wittlin, S.; Charman, S. A.; Avery, V. M.; Cho, N.; Kamaura, M. Discovery and Structure–Activity Relationships of Quinazolinone-2-Carboxamide Derivatives as Novel Orally Efficacious Antimalarials. *J. Med. Chem.*, 2021; 64(17): 12582–12602.